LETTERS

Volcanic mesocyclones

Pinaki Chakraborty[1], Gustavo Gioia[2] & Susan W. Kieffer[1]

A strong volcanic plume consists of a vertical column of hot gases and dust topped with a horizontal 'umbrella'[1]. The column rises, buoyed by entrained and heated ambient air, reaches the neutral-buoyancy level, then spreads radially to form the umbrella. In classical models of strong volcanic plumes, the plume is assumed to remain always axisymmetric and non-rotating. Here we show that the updraught of the rising column induces a hydrodynamic effect not addressed to date—a 'volcanic mesocyclone'. This volcanic mesocyclone sets the entire plume rotating about its axis, as confirmed by an unprecedented analysis of satellite images from the 1991 eruption of Mount Pinatubo[2–4]. Destabilized by the rotation, the umbrella loses axial symmetry and becomes lobate in plan view, in accord with satellite records of recent eruptions on Mounts Pinatubo, Manam, Reventador, Okmok, Chaiten and Ruang. The volcanic mesocyclone spawns waterspouts[5,6] or dust devils[6–8], as seen in numerous eruptions, and groups the electric charges about the plume to form the 'lightning sheath' that was so prominent in the recent eruption of Mount Chaiten. The concept of a volcanic mesocyclone provides a unified explanation for a disparate set of poorly understood phenomena in strong volcanic plumes[5–10].

On 12 June 1811, a volcanic vent surfaced out of the sea in the Azores archipelago. A volcanic column started to rise and was observed by a ship's captain. According to the captain[5], the column rotated on the water ''like an horizontal wheel'' and was accompanied by flashes of lightning which ''continually issued from the densest part of the volcano.'' Then the column ''rolled off in large masses of fleecy clouds, gradually expanding themselves in a direction nearly horizontal, and drawing up to them a quantity of waterspouts.'' Although the three features observed by the captain—rotation of the plume about its axis, lightning close to the column, and waterspouts (or dust devils) eccentric to the column—have variously been noted over the years[6–10], the captain's report appears to be the only account of a volcanic plume in which all of these features have been noted together. What has not been noted is that these features are characteristic of a meteorological phenomenon seemingly unrelated to volcanic plumes: the cyclonically rotating columnar vortex—or mesocyclone—of a tornadic thunderstorm[11]. Here we introduce the concept of a volcanic mesocyclone. We start by providing direct evidence of the rotation attendant on a volcanic mesocyclone.

Consider Mount Pinatubo's eruption of 15 June 1991, the only large volcanic eruption for which there exists a satellite record suitable for the analysis that follows. In that eruption, the umbrella was documented by the Geostationary Meteorological Satellite (GMS), in the form of hourly images in plan view (Supplementary Fig. 1). From these images, Holasek *et al.*[2] have extracted the contours of the edge of the umbrella at four stages, 60 min apart from one another (Fig. 1a). We have processed these contours to trace the horizontal displacement of the centre of the umbrella (if any), the rotation of the edge of the umbrella about its centre (if any), and the radial expansion of the edge of the umbrella (Fig. 1b). Our calculations show that the edge of Pinatubo's umbrella rotated about its centre[2,12]. The rate of rotation decayed from $\sim$0.5 rad h^{-1} to $\sim$0.2 rad h^{-1} over a period of 2 h (Fig. 1c). Further, a comparison of the second and third contours of Fig. 1a indicates that at some time between 14:41 and 15:41 Philippine Daylight Time (PDT), the edge of the umbrella became wavy—the umbrella took a lobate shape in plan view. We estimate the number of lobes, $N = 5$, from the contour for 16:41 PDT, by which time the amplitude of the lobes attained a value comparable to the wavelength. The number of lobes may be verified in the satellite image of Fig. 1d.

Why was Pinatubo's umbrella rotating, and why did it become lobate? We argue that (1) the rotation of an umbrella is inherited from the column, which in turn rotates because of the spontaneous development of a volcanic mesocyclone, and (2) the lobateness of an umbrella is a direct consequence of the rotation, which makes the umbrella unstable and contorts its edge.

To understand why a volcanic plume rotates, consider the development of the mesocyclone of a tornadic thunderstorm. When a vigorous updraught rises in the presence of the horizontal vortex tubes associated with the strong shear layer of an ambient wind, the updraught entrains, tilts and stretches these vortex tubes to produce a pair of counter-rotating vertical vortices[11,13]. Of these counter-rotating vertical vortices, the cyclonically rotating vortex (that is, the vortex that rotates anticlockwise in the Northern Hemisphere or clockwise in the Southern Hemisphere) is preferentially enhanced by the turning of the wind-shear vector with height—a subtle effect that is ultimately caused by the rotation of the Earth[11,13]. We propose that similar processes occur in the updraught of a volcanic column, resulting in a volcanic mesocyclone that ultimately sets the entire plume rotating (Fig. 2a). (For further discussion, see Supplementary Information.)

Besides a strong shear layer (of ambient winds), there are additional sources of localized vorticity for a volcanic mesocyclone. The periphery of a strong volcanic column is lined with the eddies of a Kelvin–Helmholtz instability, which is driven by the shear between the column and the surrounding atmosphere[1]. These eddies form horizontal vortex rings (Fig. 2b) that are frequently present in strong volcanic plumes (where the updraught velocities are as high as 600 m s^{-1} in the gas-thrust region, and 200 m s^{-1} in the convective region[1]), but not in thunderstorms (where the updraught velocities are of the order of 10 m s^{-1}, even in supercells[14]). During entrainment of ambient air, these vortex rings (as well as the intense turbulent eddies that fill a volcanic column) may act as additional sources of vorticity in the formation of a volcanic mesocyclone (Fig. 2b). Thus a volcanic mesocyclone is likely to be a more robust phenomenon than its counterpart in a thunderstorm.

A number of mechanisms[15,16] might be adduced to explain why a rotating umbrella loses axial symmetry and becomes lobate in plan view (see Supplementary Information). Here we discuss one such mechanism. We assume that the edge of the umbrella is initially circular in plan view and rotates with angular velocity Ω. Further, the thickness of the umbrella is negligible compared to the radius R, so that flow in the umbrella is quasi-two-dimensional. Under these

[1]Department of Geology, [2]Department of Mechanical Science & Engineering, University of Illinois, Urbana, Illinois 61801, USA.

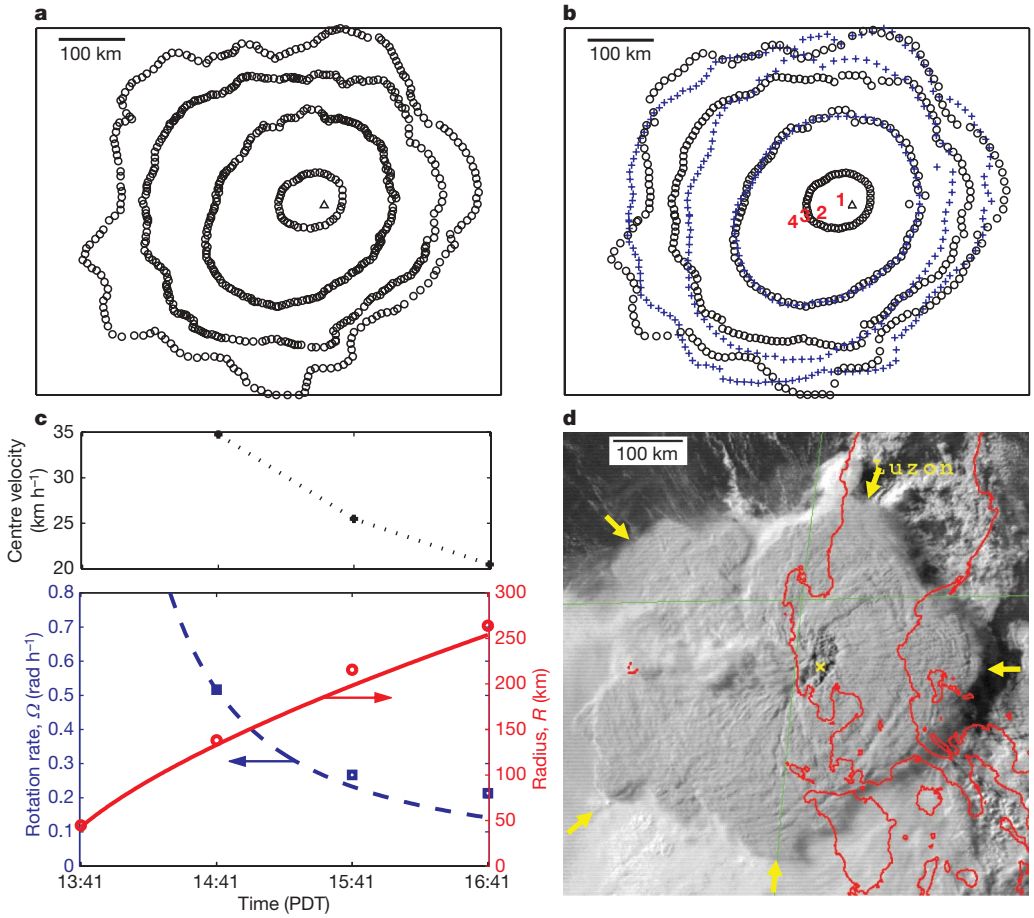

Figure 1 | Analysis of Pinatubo's umbrella (15 June 1991). **a**, Contours of the edge of Pinatubo's umbrella at hourly intervals from 13:41 PDT (the first, smallest contour) to 16:41 PDT (the fourth, largest contour); Mount Pinatubo is indicated by a triangle. (PDT, Philippine Daylight Time.) After ref. 2. **b**, Black contours (open circles) are those of **a** for 13:41, 14:41, 15:41 and 16:41 PDT. Red numbers 1 to 4 indicate the calculated centres of rotation (see below) of the black contours, starting with the black contour for 13:41, the centroid of which we take to be the centre of rotation. Blue contours (crosses) are processed contours for 14:41, 15:41 and 16:41 PDT; to obtain the processed contour for 15:41, say, we displace, rotate, and expand the black contour for 14:41 about its centre of rotation for best fit with the black contour for 15:41. (See Supplementary Information for details.) **c**, Top panel, the velocity of the centre of rotation versus time, from the analysis of satellite images. Bottom panel, the radius of the umbrella, R, versus time (red open circles) and the rate of rotation, Ω, versus time (open blue squares), from the analysis of satellite images. Solid lines are theoretical predictions for $R(t)$ (from ref. 2) and for $\Omega(t)$ (from imposing conservation of angular momentum: $\Omega(t)R(t)^2 = \text{constant} = \Omega(t = 14{:}41)R(t = 14{:}41)^2$). **d**, Satellite image of the lobate umbrella at 16:41 PDT[2–4]. Yellow arrows, location of lobes; yellow cross, location of Mount Pinatubo; red outlines, the Philippine islands including Luzon.

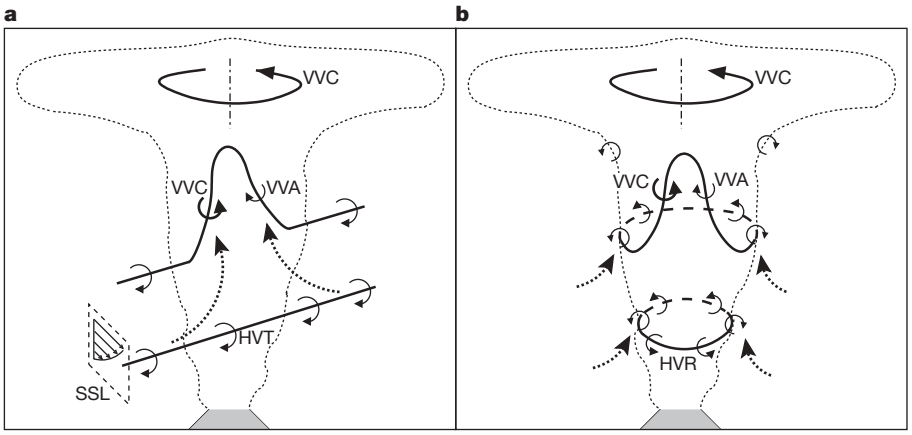

Figure 2 | Diagrams to illustrate the formation of a volcanic mesocyclone starting from different sources of vorticity (not to scale). We consider two sources: **a**, the horizontal vortex tubes (HVT) associated with the strong shear layer (SSL) of an ambient wind, and **b**, the horizontal vortex rings (HVR) associated with the Kelvin–Helmholtz instability that develops between the rising column and the surrounding atmosphere. The horizontal vortex tubes of **a** and the horizontal vortex rings of **b** are entrained, tilted and stretched by the updraught to produce counter-rotating vertical vortices in the updraught of the volcanic plume. Of the counter-rotating vertical vortices, the cyclonic vortex (VVC) becomes dominant relative to the anticyclonic vortex (VVA).

assumptions and in a frame of reference that rotates with the edge of the umbrella, the fluid in the umbrella is subjected to two radial body forces near the edge of the umbrella: a centrifugal force $\Omega^2 R$ and a Coriolis force $\pm 2\Omega u$, where u is the magnitude of the turbulent (fluctuating) fluid velocity. Near the edge of the umbrella u is tangent to the edge, and its magnitude is set by the velocity of the largest turbulent eddies, which is about 10^{-2} times the characteristic velocity of the flow[17–19]. As the characteristic velocity of the flow is ΩR, $u \approx 10^{-2}\Omega R$, and the Coriolis force has a magnitude of $\sim 2 \times 10^{-2}\Omega^2 R$. We conclude that the dominant body force near the edge of the umbrella is the centrifugal force. It is directed radially outward and has a magnitude of $\Omega^2 R$.

As the umbrella expands, the fluid near its edge cools and thus becomes denser than the surrounding atmosphere. This density contrast coupled with the centrifugal force (which is directed radially outward from the dense edge of the umbrella towards the less dense atmosphere) triggers a baroclinic instability—a turbulent, centrifugal form of the Rayleigh–Taylor instability. (In a turbulent Rayleigh–Taylor instability[20], diffusion is governed by eddy viscosity[1,21,22] as opposed to molecular viscosity.) By following steps similar to those outlined in ref. 20, we derive a mathematical relation between Ω, N, and the characteristic time of the instability, τ, where τ represents the time required for the amplitude of the lobes to attain a value comparable to the wavelength (see Supplementary Information for details):

$$\tau\Omega\sqrt{N} = 1 \quad (1)$$

From our analysis of satellite images of Pinatubo (Fig. 1a), we concluded that at some time between 14:41 and 15:41 PDT, the Pinatubo umbrella became unstable and developed $N = 5$ lobes. Therefore, the angular velocity was $\Omega \approx 0.4\ \mathrm{rad\ h^{-1}}$ when the instability was triggered (at the midpoint between 14:41 and 15:41 PDT (Fig. 1c)). From our analysis of satellite images of Pinatubo, we also concluded that at 16:41 PDT, about 1.5 h after the instability was triggered, the amplitude of the lobes attained a value comparable to the wavelength. It follows that we would expect equation (1) to give $\tau \approx 1.5$ h; substituting $\Omega = 0.4\ \mathrm{rad\ h^{-1}}$ and $N = 5$ in equation (1), we get $\tau = 1.1$ h, in reasonable accord with expectation.

As the conditions for the development of a volcanic mesocyclone are commonly realized in strong volcanic plumes, we predict that the umbrellas of such plumes usually rotate and become lobate. This prediction may be confirmed in satellite records (Fig. 3). We propose that the rotation of an umbrella and the attendant lobateness are distinctive signatures of a volcanic mesocyclone. Other signatures are the spawning of tornadoes (waterspouts on water and dust devils on land) and the formation of sheaths of lightning. We address the spawning of tornadoes first.

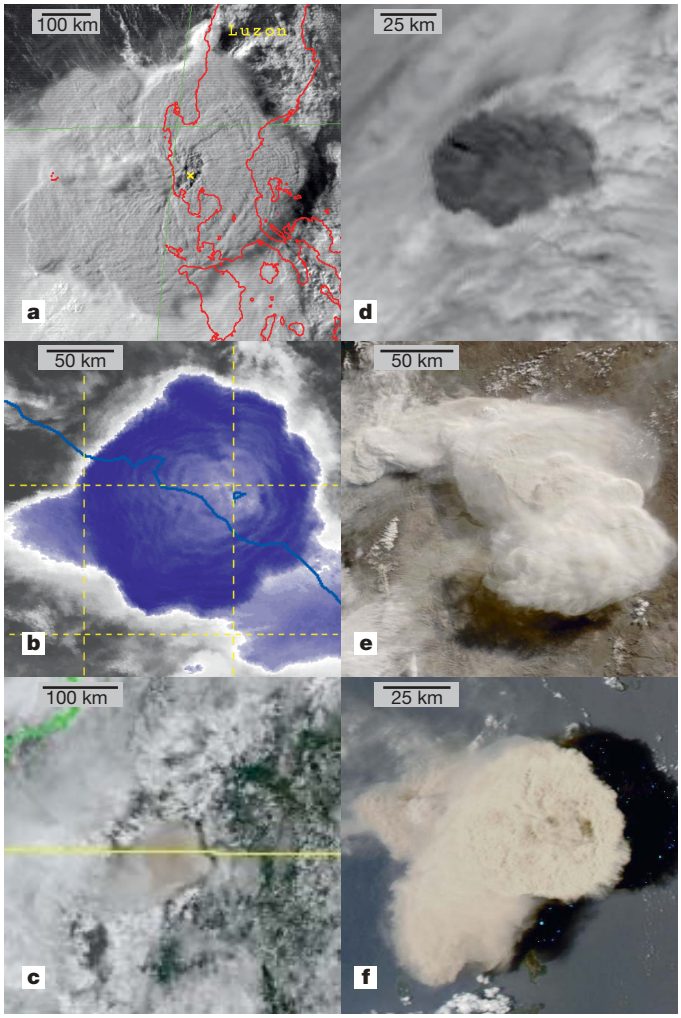

Figure 3 | Satellite images of lobate umbrellas. **a**, Pinatubo (Philippines) on 15 June 1991, 16:41 local time (diameter ~540 km); **b**, Manam (Papua New Guinea) on 27 January 2005, 15:35 UTC (180 km); **c**, Reventador (Ecuador) on 3 November 2002, 15:10 UTC (85 km); **d**, Okmok (Alaska, USA) on 12 July 2008, 20:43 UTC (~65 km); **e**, Chaiten (Chile) on 6 May 2008, 15:05 UTC (~115 km); and **f**, Ruang (Indonesia) on 25 September 2002, 04:50 UTC (~60 km). Data sources: GMS (**a**); NASA MODIS (**b**, **c**, **e**, **f**); NOAA/AVHRR (**d**).

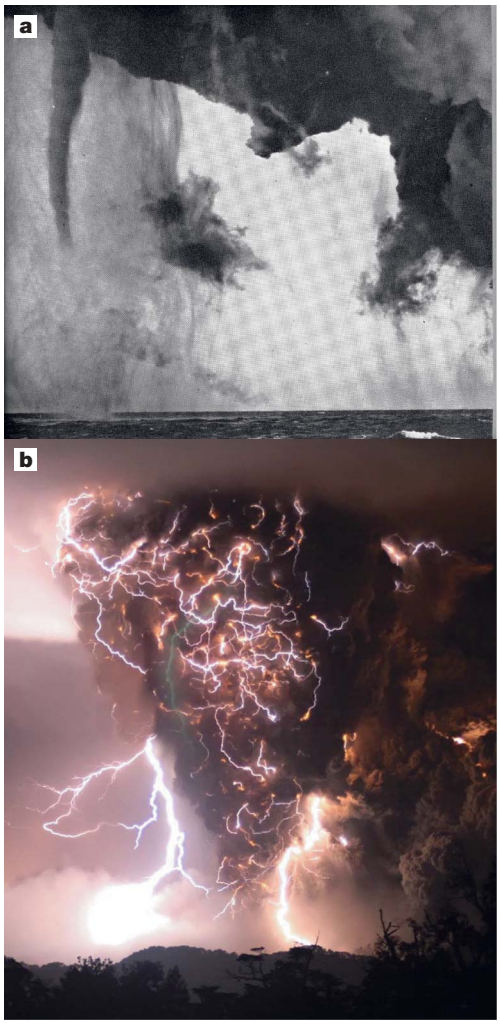

Figure 4 | Secondary signatures of a volcanic mesocyclone. **a**, Waterspouts spawned during the eruption of Surtsey volcano on 14 November 1963 (ref. 6). **b**, A lightning sheath covers the volcanic column from Mount Chaiten on 3 May 2008. (Used with permission from Landov Media.)

In a tornadic thunderstorm, the key elements that interact (in ways imperfectly understood) to yield tornadoes eccentric to the axis of the thunderstorm are ''a buoyant updraft, rainy downdrafts, and a deep, mesocyclonic vortex (preexisting vertical vorticity)''[13]. We propose that in a volcanic eruption the same elements—updraught (which has been extensively studied[1]), downdraughts (which have received little attention[23,24]) and the volcanic mesocyclone (which is the subject of this work)—yield the tornadic structures, such as dust devils and waterspouts that are frequently observed in strong volcanic plumes[5–8] (for example, Fig. 4a).

In connection with lightning[7,9,10] in strong volcanic plumes, we discuss supercells, a type of thunderstorm that might be the closest analogue to strong volcanic plumes. A supercell is a thunderstorm with an intense mesocyclone and a highly organized internal structure[14]. Within the swift updraught of a supercell there is insufficient time for a sizable amount of precipitation to form, grow and gain charge via collisions[25,26]. As a result, lightning remains minimal within the updraught of a supercell, and the core of the updraught has been termed a 'lightning hole'[25–27]. It has recently been proposed that in supercells the mesocyclone pulls the precipitation radially outwards from the core of the updraught, gathering the precipitation over the periphery of the updraught, where it sets up the formation of a 'lightning sheath' (or 'ring'[28]) around the updraught[29]. Remarkably, photographs from the recent eruption of Chaiten (for example, Fig. 4b) show the surface of the volcanic column prominently coated in a layer of lightning, which we identify as a lightning sheath.

We have argued that strong volcanic plumes are accompanied by volcanic mesocyclones. Signatures of a volcanic mesocyclone include a rotating plume, a lobate umbrella, the spawning of tornadoes, and the formation of a lightning sheath and hole. These signatures, which remain unaccounted for in current models, must be present in most strong volcanic plumes, even though they may be obscured by distorting winds and other phenomena unrelated to the volcanic eruption. We hope that these signatures will be the subject of future remote sensing observations and field work on volcanic plumes. Satellite images at intervals of a few minutes would make it possible to trace the evolution of umbrellas in detail. The structure and dynamics of volcanic mesocyclones, as well as the presence of lightning sheaths and holes, might be verified using respectively Doppler radar[30] and lightning mapping arrays[10], two technologies that have been scarcely used in volcanology. Last, we hope that the concept of a volcanic mesocyclone will help us forecast, and alleviate, the impact of volcanic eruptions.

Received 16 October 2008; accepted 11 February 2009.

1. Sparks, R. S. J. *et al. Volcanic Plumes* (Wiley and Sons, 1997).
2. Holasek, R. E., Self, S. & Woods, A. W. Satellite observations and interpretations of the 1991 Mount Pinatubo eruption plumes. *J. Geophys. Res.* **101,** 27635–27655 (1996).
3. Oswalt, J. S., Nichols, W. & O'Hara, J. F. in *Fire and Mud: Eruptions and Lahars of Mount Pinatubo, Philippines* (eds Newhall, C. G. & Punongbayan, R. S.) 625–636 (Philippine Institute of Volcanology and Seismology and University of Washington Press, 1996).
4. Self, S., Zhao, J., Holasek, R. E., Torres, R. C. & King, A. in *Fire and Mud: Eruptions and Lahars of Mount Pinatubo, Philippines* (eds Newhall, C. G. & Punongbayan, R. S.) 1089–1115 (Philippine Institute of Volcanology and Seismology and University of Washington Press, 1996).
5. Tillard, S. A narrative of the eruption of a volcano in the sea off the island of St. Michael. *Phil. Trans. R. Soc. Lond. B* **102,** 152–158 (1812).
6. Thorarinsson, S. & Vonnegut, B. Whirlwinds produced by the eruption of Surtsey volcano. *Bull. Am. Meteorol. Soc.* **45,** 440–444 (1964).
7. Anderson, R. *et al.* Electricity in volcanic clouds: investigations show that lightning can result from charge-separation processes in a volcanic crater. *Science* **148,** 1179–1189 (1965).
8. Stothers, R. B. The great Tambora eruption in 1815 and its aftermath. *Science* **224,** 1191–1198 (1984).
9. Mather, T. A. & Harrison, R. G. Electrification of volcanic plumes. *Surv. Geophys.* **27,** 387–432 (2006).
10. Thomas, R. J. *et al.* Electrical activity during the 2006 Mount St. Augustine volcanic eruptions. *Science* **315,** 1097 (2007).
11. Klemp, J. B. Dynamics of tornadic thunderstorms. *Annu. Rev. Fluid Mech.* **19,** 369–402 (1987).
12. Baines, P. G. & Sparks, R. S. J. Dynamics of giant volcanic ash clouds from supervolcanic eruptions. *Geophys. Res. Lett.* **32,** L24808, doi:10.1029/2005GL024597 (2005).
13. Davis-Jones, R., Trapp, R. J. & Bluestein, H. B. in *Severe Convective Storms* Ch. 5 (ed. Doswell, C. A. III) 167–221 (Meteorological Monographs Vol. 28, American Meteorological Society, 2001).
14. Emanuel, K. *Atmospheric Convection* (Oxford Univ. Press, 1994).
15. Griffiths, R. W. Gravity currents in rotating systems. *Annu. Rev. Fluid Mech.* **18,** 59–89 (1986).
16. Linden, P. F. in *Rotating Fluids in Geophysical and Industrial Applications* (ed. Hopfinger, E. J.) 99–123 (Springer, 1992).
17. Tennekes, H. & Lumley, J. L. *A First Course in Turbulence* (MIT Press, 1972).
18. Landau, L. D. & Lifshitz, E. M. *Course of Theoretical Physics* Vol. 6, *Fluid Mechanics* (Elsevier Academic Press, 2000).
19. Gioia, G. & Chakraborty, P. Turbulent friction in rough pipes and the energy spectrum of the phenomenological theory. *Phys. Rev. Lett.* **96,** 044502 (2006).
20. Chakraborty, P., Gioia, G. & Kieffer, S. Volcan Reventador's unusual umbrella. *Geophys. Res. Lett.* **33,** L05313, doi:10.1029/2005GL024915 (2006).
21. Valentine, G. A. & Wohletz, K. H. Numerical models of plinian eruption columns and pyroclastic flows. *J. Geophys. Res.* **94,** 1867–1887 (1989).
22. Pedlosky, J. *Geophysical Fluid Dynamics* (Springer, 1979).
23. Hoblitt, R. P. Was the 18 May 1980 lateral blast at Mt. St. Helens the product of two explosions? *Phil. Trans. R. Soc. Lond. A* **358,** 1639–1661 (2000).
24. Tupper, A., Oswalt, J. S. & Rosenfeld, D. Satellite and radar analysis of the volcanic-cumulonimbi at Mt Pinatubo, Philippines, 1991. *J. Geophys. Res.* **110,** D09204, doi:10.1029/2004JD005499 (2005).
25. MacGorman, D. R. *et al.* The electrical structure of two supercell storms during STEPS. *Mon. Weath. Rev.* **133,** 2583–2607 (2005).
26. Wiens, K. C., Rutledge, S. A. & Tessendorf, S. A. The 29 June 2000 supercell observed during STEPS, part II: Lightning and charge structure. *J. Atmos. Sci.* **62,** 4151–4177 (2005).
27. Krehbiel, P. R. *et al.* GPS-based mapping system reveals lightning inside storms. *Eos* **81,** 21–25 (2000).
28. Payne, C. *The Evolution of a Lightning Hole during the 29–30 May 2004 HP Supercell during TELEX.* M.Sc. thesis, Univ. Oklahoma (2008).
29. Bruning, E. *Charging Regions, Regions of Charge, and Storm Structure in a Partially Inverted Polarity Supercell Thunderstorm*. Ph.D. thesis, Univ. Oklahoma (2008).
30. Dubosclard, G. *et al.* First testing of a volcano Doppler radar (VOLDORAD) at Mount Etna, Italy. *Geophys. Res. Lett.* **26,** 3389–3392 (1999).

Supplementary Information is linked to the online version of the paper at www.nature.com/nature.

Acknowledgements We acknowledge discussions with A. Tupper, D. MacGorman, S. Nesbitt and M. Fromm. We thank the members of the 'volcanic clouds' discussion list for help with satellite images. P.C. and S.W.K. acknowledge support through the latter's Walgreen Chair funds and NSF\EAR grant 06-09712 (S. Esperanza, programme director). G.G. acknowledges support through NSF\DMR grant 06-04435 (W. Fuller-Mora, programme director).

Author Information Reprints and permissions information is available at www.nature.com/reprints. Correspondence and requests for materials should be addressed to P.C. (chakrabo@illinois.edu).

Supplementary Discussion

Analysis of umbrellas: displacement, rotation, and expansion

The aim of this analysis is to obtain the following values (as a function of time) during the evolution of the umbrella: the horizontal displacement of the centre of rotation of the umbrella, the rotation of the edge of the umbrella, and the radial expansion of the edge of the umbrella. The data for this analysis are the digitised contours (in Cartesian coordinates (x, y)) of the edge of Pinatubo's umbrella (the black contours in open circles in Fig. 1a and b) at intervals of 1 h. To reduce the affects of noise in the data on the results of the analysis, we smoothen the contours using undersampling and then interpolate the contours using cubic splines. To illustrate the steps in the analysis, consider the step from 14:41 to 15:41 PDT. We apply the following transformations to the contour of 14:41:

- Displace the centre of rotation of the contour by a displacement u km in the x direction and a displacement v km in the y direction. (The centre of rotation is obtained from the preceding step. For the start of the analysis—the step from 13:41 to 14:41—we take the centroid of the contour of 13:41 to be its centre of rotation.)

- Rotate the contour by an angle θ rad about the displaced centre of rotation.

- Radially expand the displaced and rotated contour about the displaced centre of rotation. To that end, multiply by a factor α the distance of each point on the displaced and rotated contour from the displaced centre of rotation.

The above transformations give us a displaced, rotated, and expanded contour of 14:41 as a function of u, v, θ and α. To obtain the values of u, v, θ and α, we perform a non-linear curve fitting by minimising the least-squares error between the displaced, rotated, and expanded contour of 14:41 and the contour of 15:41. The least-squares vector is composed of the radial distance between each point of the displaced, rotated, and expanded contour of 14:41 and the corresponding point from the contour of 15:41. The non-linear curve fitting is a four-dimensional least-squares problem. We use the MATLAB Optimisation Toolbox function "lsqnonlin" with large-scale algorithm to solve the non-linear least squares problem. From this analysis of the satellite images we obtain the values of velocity of the centre of rotation ($\sqrt{u^2+v^2}/1$ h), rate of rotation ($\theta/1$ h), and radius ($\alpha \times$ previous radius) shown in Fig. 1c. (The radius of the first contour is the average distance between the points of the first contour and its centroid.) In the analysis, the maximum error is for the value of the rate of rotation for the step from 14:41 to 15:41. This is because the contour of 14:41 has no lobes and the contour of 15:41 is lobate.

Rotating Umbrella

* Angular momentum in a volcanic mesocyclone

The angular momentum per unit mass in the mesocyclone of a typical thunderstorm[1,2] is $0.25\,\mathrm{km}^2/\mathrm{s}$ (radius $R = 5$km and rotation rate $\Omega = 0.01$rad/s). By comparison, in the Pinatubo umbrella the angular momentum per unit mass is $\Omega(t)R(t)^2 = 2.5\,\mathrm{km}^2/\mathrm{s}$ (see caption of Fig. 1c), an order of magnitude larger than in the mesocyclone of a typical thunderstorm.

* Volcanic plume vs. hydrothermal plume

It is instructive to compare rotating volcanic plumes with rotating hydrothermal 'event' plumes from the seafloor [3,4]. A hydrothermal plume develops over a time scale of many hours to a few days, and its rotation is governed by the Coriolis forces from Earth's rotation [3,5,6]. By contrast, a volcanic mesocyclone develops over a time scale of a few hours, and its rotation remains unrelated to the Coriolis forces from Earth's rotation. The effect of these Coriolis forces become manifest over time scales of about 24 hours [3,5,6]. In the case of a hydrothermal plume, as in the case of a tropical cyclone[7], modulations by the Coriolis forces results in a dichotomy of rotation: cyclone at lower level and anticyclone at spreading level [3,5]. By contrast, a volcanic mesocyclone makes the whole volcanic plume rotate only cyclonically.

* Rotation in other plumes

The mechanism of production of vertical vorticity in a mesocyclone (thunderstorm and volcanic) involves entrainment, tilting, and stretching of vortex tubes from the shear layer of the ambient wind. This mechanism is also responsible for the production of vertical vorticity in many other types of plume, for example in fire storms[8] and thermal plumes in turbulent convection[9].

Instabilities in a Rotating Umbrella

As pointed out in the paper, the lobateness of the umbrella is a manifestation of an instability triggered by the rotation of the umbrella. This instability might be governed by a number of mechanisms. In the paper we have focused on one baroclinic mechanism that seems most plausible to us: a centrifugal version of a turbulent Rayleigh–Taylor instability. For the prevailing conditions of the Pinatubo umbrella, this mechanism gives predictions for the wavelength (or number of lobes) and the characteristic time of the instability, that are in good accord with our analysis of the satellite images of Pinatubo's eruption. Here we outline briefly some other mechanisms that

might be invoked to explain the lobateness of a rotating umbrella. In all of these mechanisms the umbrella is construed as an axisymmetric gravity current whose circular front expands radially, while the entire gravity current rotates about its axis.

In a typical experimental setup to study axisymmetric rotating gravity currents[10–13], a constant volume or a constant flux of a buoyant (or denser) quiescent fluid is released close to the axis of rotation into a stratified or homogeneous ambient fluid that is in solid-body rotation with a constant angular velocity Ω. As the quiescent fluid spreads radially with a circular front as a gravity current, it develops an anticyclonic rotation (as opposed to an umbrella, which remains in cyclonic rotation from the beginning of the radial spreading). After a time comparable to few times the revolution time, $2\pi/\Omega$, the initially circular front becomes unstable and develops lobes. These lobes grow in time to result in large-amplitude structures, which may break off from the main flow to form eddies. The instability that makes the circular front lobate might be governed by a number of mechanisms. Near the front, the flow may be ageostrophic and become unstable under weaker conditions than a quasi-geostrophic flow[12]. The instability mechanisms—barotropic, baroclinic, combination of barotropic and baroclinic, resonance between Rossby waves and gravity waves, etc—depend on the details of the flow[12–14]. One parameter that characterises the instability mechanism is the ratio of the internal Rossby radius of deformation, λ_0. and the initial radius of the spreading fluid, R_0. For example, when the ratio $\lambda_0/R_0 < 1$, the instability is dominated by baroclinic effects and the dominant wavelength of the instability is a constant multiple of λ_0.

An additional consideration for the instability in a rotating umbrella is the role of gravity waves. Gravity waves, which are frequently observed in volcanic umbrellas[15,16], were prominent in the satellite images of the Pinatubo umbrella[17–19]. These waves might play a role in the instability of a rotating umbrella. In particular, the resonance between the gravity waves in a rotating umbrella and the Rossby waves may trigger the Rossby–Kelvin instability to make the umbrella lobate [13,14].

How are the experiments described above related with the instability in a rotating umbrella? An ideal experiment to simulate the instability in a rotating umbrella would consist of releasing a constant flux of a denser rotating fluid in a quiescent stratified ambient fluid. We are not aware of any such experiments. Since the instability mechanisms in rotating gravity currents depend on the details of the flow, the wavelength and timescale of the instability in a rotating umbrella may be different from that of the experiments described above. One notable difference in the experiments described above and rotating umbrellas is the absence of breaking off of eddies from the umbrella. This difference may be attributed to the fact that the rate of rotation of the spreading umbrella decreases with time (see Fig. 1c in the paper), whereas the experiments described above that have a constant rate of rotation.

To the extent that one may apply the results from the instability of rotating gravity currents to rotating umbrellas, now we estimate the the ratio λ_0/R_0 that characterises the instability mechanism for the case of Pinatubo's umbrella. To estimate the value of λ_0, we use its definition[12,13,20]:

$$\lambda_0 = \frac{N_s h_0}{2\Omega},$$

where N_s is the buoyancy frequency and h_0 is the initial thickness of the spreading umbrella. For the Pinatubo umbrella, using[17,21] $N_s = 0.017\text{s}^{-1}$, $h_0 = 5\,\text{km}$ (the value of h_0 may be as high as $10\,\text{km}$ [21]), and $\Omega = 5\,\text{rad/h}$ (using the theoretical estimate of Ω at time 13:41 PDT; see Fig. 1c in the paper), we find $\lambda_0 \approx 30\,\text{km}$. The ratio of λ_0 and the initial radius of the umbrella ($R_0 \approx 50\,\text{km}$ at time 13:41 PDT; see Fig. 1c in the paper) is 0.6; hence, we expect a baroclinic instability to dominate the lobateness of the Pinatubo umbrella. Interestingly, in the paper we discuss a baroclinic instability—a centrifugal version of a turbulent Rayleigh–Taylor instability—to explain lobateness in Pinatubo's umbrella and other rotating umbrellas in general.

Turbulent Rayleigh–Taylor instability

A turbulent Rayleigh–Taylor instability is driven by an acceleration g (usually the gravitational acceleration) that acts perpendicular to an interface with a density contrast and points in the direction of decreasing density. The rate of growth of this instability is maximum for a wavelength[22]

$$\lambda \approx 2\pi \frac{\nu_e^{2/3}}{g^{1/3}},$$

with an associated characteristic time for this wavelength[22].

$$\tau \approx \frac{\nu_e^{1/3}}{g^{2/3}}.$$

For a centrifugal, turbulent form of the Rayleigh–Taylor instability that develops at the edge of an umbrella of radius R, we replace the body force g by $\Omega^2 R$. To estimate the value of the eddy viscosity, ν_e, recall that the velocity and size of the largest eddies, V_e and l, are $V_e = \kappa \Omega R$ and $l = cR$, where $\kappa \approx 10^{-2}$ and c is a dimensionless proportionality constant. It follows[23] that $\nu_e \approx V_e l = \kappa c \Omega R^2$. By substituting these expressions in the equations for λ and τ, we get:

$$N \approx (\kappa c)^{-2/3} \quad \text{and} \quad \tau \approx \frac{(\kappa c)^{1/3}}{\Omega},$$

where $N \equiv 2\pi R/\lambda$ is the number of lobes in the umbrella. By eliminating the constant c from the expressions for N and τ, we get equation (1) of the paper.

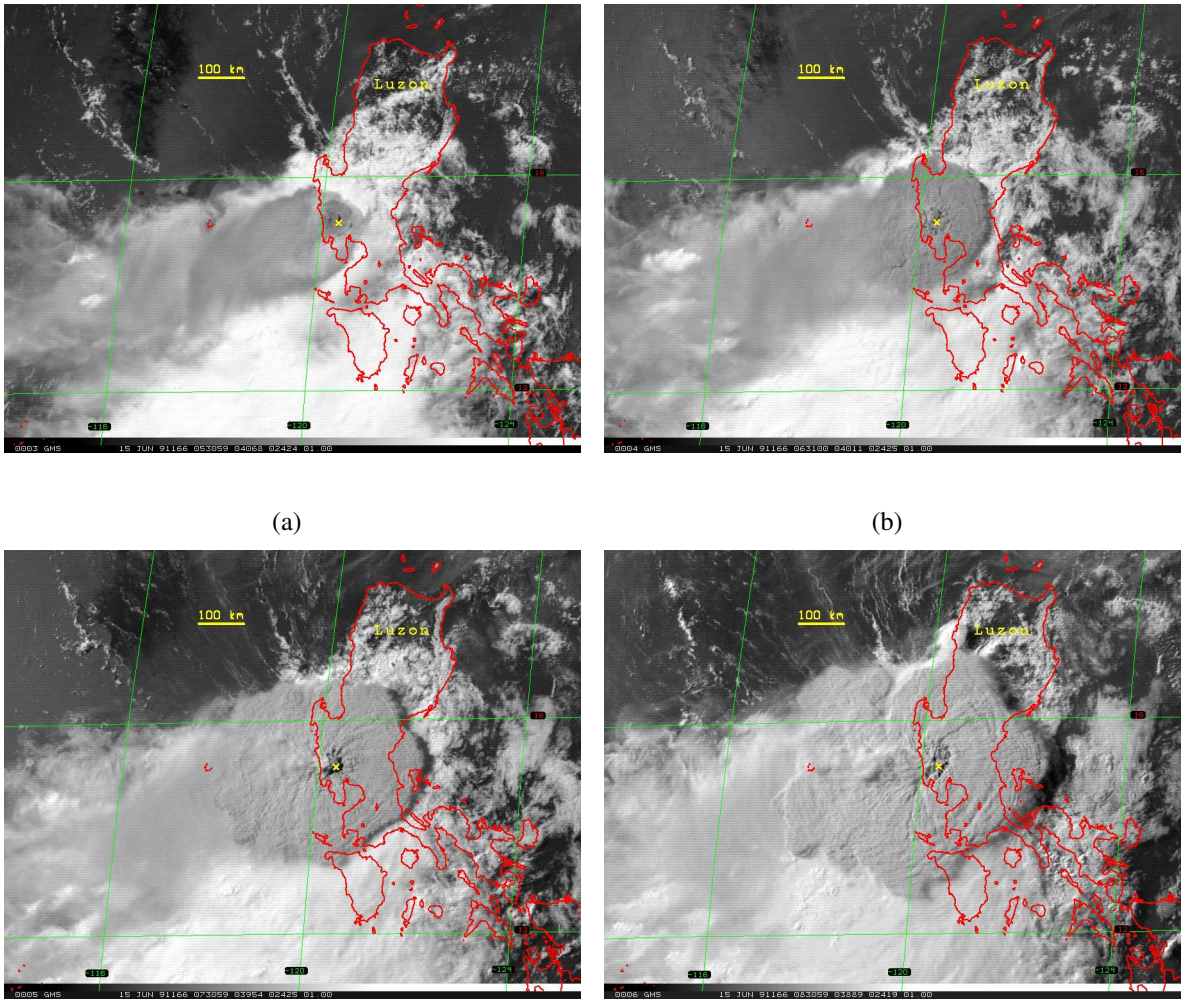

Figure S-1: Hourly GMS images of Mount Pinatubo's climactic eruption[17,18,24] on 15 June 1991: from 13:41 PDT (frame a) to 16:41 PDT (frame d).

1. *Glossary of Meteorology* (American Meteorological Society, 2000).

2. Davis-Jones, R., Trapp, R. J. & Bluestein, H. B. Tornadoes and tornadic storms. In Doswell III, C. A. (ed.) *Severe Convective Storms*, vol. 28 of *Meteorological Monographs* (American Meteorological Society, 2001).

3. Speer, K. G. A New Spin on Hydrothermal Plumes. *Science* **280**, 1034–1035 (1998).

4. Lupton, J. E. *et al.* Tracking the Evolution of a Hydrothermal Event Plume with a RAFOS Neut rally Buoyant Drifter. *Science* **280**, 1052–1055 (1998).

5. Helfrich, K. R. & Speer, K. G. Oceanic hydrothermal circulation: Mesoscale and basin-scale flow. In *Seafloor Hydrothermal Systems: Physical, Chemical, Biological, and Geological Interactions*, vol. 91 of *Geophysical Monograph*, 347–356 (American Geophysical Union, 1995).

6. Bush, J. W. M. & Woods, A. W. Experiments on buoyant plumes in a rotating channel. *Geophys. Astrophys. Fluid Dynamics* **89**, 1–22 (1998).

7. Emanuel, K. *Divine Wind: The History and Science of Hurricanes* (Oxford University Press, 2005).

8. Morton, B. R. The physics of fire whirls. In *Fire Research Abstracts and Reviews*, vol. 12, 1–19 (1970).

9. Cortese, T. & Balachandar, S. Vortical nature of thermal plumes in turbulent convection. *Phys. Fluids A* **5**, 3226–3232 (1993).

10. Griffiths, R. W. & Linden, P. F. The stability of vortices in a rotating, stratified fluid. *J. Fluid Mech.* **105**, 283–316 (1981).

11. Griffiths, R. W. & Linden, P. F. Laboratory experiments on fronts. Part I. density-driven boundary currents. *Geophys. Astrophys. Fluid Dyn.* **19**, 159–187 (1982).

12. Griffiths, R. W. Gravity currents in rotating systems. *Ann. Rev. Fluid Mech.* **18**, 59–89 (1986).

13. Linden, P. F. *Rotating Fluids in Geophysical and Industrial Applications*, chap. Dynamics of Fronts and Frontal Instability, 99–123 (Springer–Verlag, 1992).

14. Sakai, S. Rossby–Kelvin instability: a new type of ageostrophic instability caused by a resonance between Rossby waves and gravity waves. *J. Fluid Mech.* **202**, 149–176 (1989).

15. Carey, S. & Sigurdsson, H. The 1982 eruptions of El Chichon volcano, Mexico (2): Observations and numerical modelling of tephra-fall distribution. *Bull. Volcanol.* **48**, 127–141 (1986).

16. Textor, C. *et al.* Volcanic particle aggregation in explosive eruption columns. Part I: Parameterization of the microphysics of hydrometeors and ash. *Journal of Volcanology and Geothermal Research* **150**, 359–377 (2006).

17. Holasek, R. E., Self, S. & Woods, A. W. Satellite observations and interpretations of the 1991 Mount Pinatubo eruption plumes. *J. Geophys. Res.* **101**, 27635–27655 (1996).

18. Oswalt, J. S., Nichols, W. & O'Hara, J. F. *FIRE and MUD: Eruptions and Lahars of Mount Pinatubo, Philippines*, chap. Meteorological Observations of the 1991 Mount Pinatubo Erup-

tion (Philippine Institute of Volcanology and Seismology and University of Washington Press, 1996).

19. Lynch, J. S. & Stephens, G. *FIRE and MUD: Eruptions and Lahars of Mount Pinatubo, Philippines*, chap. Mount Pinatubo: A Satellite Perspective of the June 1991 Eruptions (Philippine Institute of Volcanology and Seismology and University of Washington Press, 1996).

20. Pedlosky, J. *Geophysical Fluid Dynamics* (Springer–Verlag, 1979).

21. Koyaguchi, T. Grain-size variation of tephra derived from volcanic umbrella clouds. *Bull. Volcanol.* **56**, 1–9 (1994).

22. Chakraborty, P., Gioia, G. & Kieffer, S. Volcan Reventador's unusual umbrella. *Geophys. Res. Lett.* **33**, L05313 (2006).

23. Landau, L. D. & Lifshitz, E. M. *Fluid Mechanics*, vol. 6 of *Course of Theoretical Physics* (Elsevier Academic Press, 2000).

24. Self, S., Zhao, J., Holasek, R. E., Torres, R. C. & King, A. *FIRE and MUD: Eruptions and Lahars of Mount Pinatubo, Philippines*, chap. The Atmospheric Impact of the 1991 Mount Pinatubo Eruption (Philippine Institute of Volcanology and Seismology and University of Washington Press, 1996).